Anal. Bioanal. Electrochem., Vol. 11, No. 2, 2019, 267-277

Analytical &
Bioanalytical
Electrochemistry

Full Paper

Development of On-step Electrochemical Synthesis to Fabricate Three-dimensional N-doped Porous Graphene/magnetic Nanocomposite as novel superparamagnetic material for bio-medicinal uses

Morteza Rezapour*

IP Department, Research Institute of the Petroleum Industry (RIPI), P.O. Box 14665-137, Tehran, Iran

*Corresponding Author, Tel.: +98 21 48252228; Fax: +98 21 44739778

E-Mail: Rezapourm@ripi.ir

Received: 27 October 2018 / Received in revised form: 7 January 2019 / Accepted: 17 January 2019 / Published online: 28 February 2019

Abstract- In this paper, a novel nanocomposite based on the magnetite nanoparticles and three-dimensional nitrogen doped porous graphene was fabricated. In this way, a typical galvanostatic electrosynthesis was carried out in the aqueous bath with composition of Mn chloride, ion chloride, iron nitrate and nitrogen doped porous graphene. The XRD data proved the magnetite phase of the deposited iron oxide onto nitrogen doped porous graphene. It is also observed that the fabricated sample has composed of Fe_3O_4 nanoparticles with Mn^{2+} doped cations in their crystal structures. VSM measurements indicated that the Mn doped iron oxide/ nitrogen doped porous graphene composite exhibits superparamagnetic behavior, and have saturation magnetization, remanence magnetization and coercivity of *Ms*=33.45 emu g^{-1}, *Mr*=0.26 emu g^{-1} and *Hci*=2.41G, respectively. Compared with naked iron oxide and metal-ion doped iron oxide nanoparticles, the composite showed better superparamagnetic performance (i.e. lower *Hci* and *Mr*), which was related to well-dispersion of particles onto porous graphene and their single domain magnetic behavior.

Keywords- Iron oxide; manganese doping; N doped graphene; Electrochemical deposition; Nanocomposite

1. INTRODUCTION

Graphene and its related compounds are promising materials for various applications in the fields of optical/electrochemical sensors, energy storage, catalyst, sensor, bio-imaging, electronic devices and etc. [1-7]. This is due to their unique electrochemical, optical, electrical, chemical and electronic capabilities [8]. Graphene and its derivatives could be bio-functionalized with various bio-molecules, where the improvements in their stability, solubility, biocompatibility, and selectivity are observed [9-11]. In the graphene-based nanomaterials, properties like as π–π stacking and electrostatic interactions and large specific area simplify soluble drugs loading and provide high efficiency and validity in delivery of the loaded molecules [١٢].

In the last decade, nanostructured metal oxides and their composites have been intensively investigated and their various potential uses like as electrocatalyst, energy storage, biomedicine, and sensing have been evaluated [13-25]. In this regard, magnetic nanomaterials including metal/metal oxides have been recently received great attention to use in the different fields of bio-medicine, dye removal, electrocatalyst, supercapacitors, batteries and etc. [26-31]. Among magnetic nano-oxides, iron-based oxides i.e. magnetite, hematite and maghemite have been proven to be the best candidate for use in these areas [32,33]. This is due to their low cost, proper magnetic behavior, high porosity, various oxidation states, large specific surface area, and strong magnetic response.

Moreover, it has been also mentioned that the combination of magnetic material and graphene could be enhanced the fabricated nanocomposite performance in the above mentioned applications [34-36]. In fact, the combination of magnetite nanoparticles (NPs) with carbon-based nanostructures has recently fascinated huge research in bio-medicine due to the formed nanocomposite enable to refine the problems related to the naked iron oxide NPs and show the intrinsic capabilities of both constitutive parts [36,37]. In this regard, iron oxide-graphene nanocomposites have been intensively studied for use in bio-medical experiments [38-40]. The controlled dispersion of Fe_3O_4 NPs onto the any form of graphene sheets/layers (e.g. porous graphene, graphene oxide, S,N doped graphene and reduced graphene oxide) opens the new window to fabricate the nano-composite materials with excellent synergetic performances in the mentioned bio-applications for magnetite NPs, i.e. in both diagnostic and therapeutic fields [41]. For instance, nanocomposite of Fe_3O_4 NPs/GO has been used at T2 contrast agent in the magnetic resonance imaging of in-vivo and non-invasive cells, and a good signal enhancement has been observed [42]. Moreover, graphene related derivatives have been used as bio-delivery carriers for cancer therapy in the in vitro controlled drug loading and targeted treatments. For example, a superparamagnetic GO–Fe_3O_4 nanocomposite has been applied is used as the delivery carrier into tumour cells, and its wad found that he high SA of graphene provides efficient drug carriers by magnetite nanoparticles [43,44]. Hence, graphene-based composites with magnetic nanoparticles have attracted research trends in the last few years.

Up now, a variety of chemical-, physical- and electrochemical-based procedures have been developed to fabricate the magnetite nanoparticles, which include solvothermal, hydrothermal, precipitation and electrochemical methods. As an easy method, electrodeposition route (both anodic and cathodic depositions) has been applied in the preparation of iron oxide nanoparticles [45-55].

Here, fabrication of $Fe^{(II)}_{1-x}Mn_xFe^{(III)}_2O_4$ /N-doped graphene composite (M-IO/NG) is reported for the first time. M-IO/NG nanocomposite is synthesized through cathodic electrochemical preparation. This procedure is based on the reductive deposition due to base generation on the cathode electrode [56-58]. The prepared nanocomposite is analyzed via X-ray diffraction, infra-red spectroscopy, scanning microscopy and vibrating sample magnetometry methods to specify its composition, crystal structure, morphology and magnetization. The obtained results are reported and discussed.

2. EXPERIMENTAL PROCEDURE

2.1. Preparation of composite

Electrochemical syntheses were carried out in classical two-electrode cell. The cathode electrode consisted of a copper plate (size of 5cm*5cm) with a geometric area of 50 cm^2. The anode section included two parallel steel sheet located in both sides of copper electrode. The graphite electrodes have identical size with copper plate i.e. a geometric area of 50 cm^2. The materials used in the experiments were $MnCl_2.6H_2O$ (Merck, purity=99.5%), $FeCl_2.4H_2O$ (Merck, purity= 99%), H_2SO_4 (Merck, 98%), $KMnO_4$ (Merck, 99.8%), H_3PO_4 (Merck, 85%), H_2O_2 (Merck, 30%) and $Fe(NO_3)_3.9H_2O$ (Merck, purity= 99.9%). GO was prepared according to the improved procedure reported by Marcano et al. [59]. Briefly, a solution of 1.5 g graphite powder, 150 mL H_2SO_4, 20 mL phosphoric acid was prepared, then 9g KMnO4 was gradually added into this solution and stirred for 12 h at 50 °C. After that the solution was cooled to T=25ºC, and poured onto 500 g ice. In final, 6ml H_2O_2 was added to the solution and its color was changed to bright yellow. After synthesis of GO, the N-doped graphene was prepared using the prepared GO via the method reported in Ref. [60]. Briefly, 50 mL of GO aqueous suspension (pH=8) was mixed with 100 mg urea. Then, the stable mixture was sealed in a Teflon-lined autoclave and hydrothermally treated at 200ºC for 12 h. After the autoclave were cooled to T=25ºC, the resulted hydrogels were washed by deionized H_2O for several times and freeze dried for 2 days. The final product was three-dimensional nitrogen-doped graphene (3D-NG).

For synthesis of composite, the following procedure was used to prepare electrolyte bath. First, Fe(III) nitrate (0.2 M), Fe(II) chloride (0.05M) and Mn chloride (0.05 M) were dissolved in 500 mL deionized H_2O. Second, 50 mg 3D-NG was added into the mixture and sonicated for 20 min. Third, the solution was stirred for 3h at T=60ºC. This prepared electrolyte was

added into the electrochemical cell as deposition bath in the syntheses runs. For the electrochemical deposition, the dc current of 0.5 A was applied into the above mentioned electrochemical cell for 30 min, and the black product was observed on the cathode side (i.e. steel sheet). Then, the product was collected form the cathode surface and washed with EtOH, and dried at 70^{o}C for 120 min in vacuum oven. The final product was named Mn-IO/3D-NG sample.

2.2. Characterizations

The surface morphologies of the synthesized Mn-IO/3D-NG sample were investigated by a Mira 3-XMU field-emission scanning electron microscope (FE-SEM, TESCAN, Czech Republic) operating at 30 kV. A Bruker Vector 22 Fourier transformed infrared (FT-IR) spectroscope was used to provide the IR spectrum of sample in the wavenumber range of 400 to 4000 cm−1. The XRD pattern of the prepared composite was recorded via X-ray diffraction (XRD, Phillips PW-1800). Using the 7400 series vibrating sample magnetometer (VSM, Lake Shore), the magnetization behavior of the fabricated sample was evaluated and the magnetic parameters of saturation magnetization, coercivity and remanent magnetization were specified.

3. RESULTS AND DISCUSSION

Fig. 1 indicates X-ray diffraction pattern of the manganese doped iron oxide nanoparticles deposited onto 3D N-doped graphene. In this pattern the well-distinct peaks related to the crystal planes of (111), (220), (311), (400), (422), (511), (440), (620), (622) and (533) are observed. These indices are in a good coincided with those of magnetite with cubic spinel structure (JCPDS number of 01-088-0315). No additional diffraction is seen, revealing the prepared nanoparticles have crystallized in the magnetite phase. Notably, Mn doping has no essential change in the XRD peaks of magnetite, as reported in the literature [61,62]. Hence, the observed XRD peaks confirmed the magnetite phase for the prepared iron oxide-based powder.

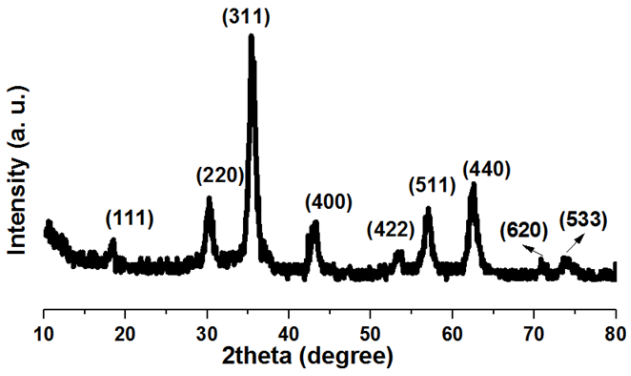

Fig. 1. XRD pattern of the synthesized composite

Morphological observations (FE-SEM images) and elemental analysis data of the prepared N-doped graphene and the composite sample (Mn^{2+} doped Fe_3O_4/3D-NG) are given in Fig. 2. For N-doped graphene, the three-dimensional porous flaky like sheets are observed (Fig. 2a). The composite sample is also exhibited particle-like sphere morphology (Figs. 2 b and c). The size of the observed particles are in the range of 20-30 nm. The elemental analysis profile of Mn-IO/3D-NG sample is also shown in Fig. 2d. For this sample, the presence of various elements including manganese, iron, oxygen, carbon and nitrogen were detected. In fact, the composite sample exhibits 7.05% wt. Mn element in this chemical composition (Fig. 2e), revealing the doping of iron oxide with manganese cations during their deposition from Mn chloride containing bath. Furthermore, this sample has 12.66%wt. carbon atoms in its composition indicating the presence of graphene in its structure. Also, nitrogen atoms with percentage of 2.66%wt. are detected in the sample (Fig. 2e), which reveals the doping of graphene layers with N atoms. Beside the N, C and Mn elements, the iron atoms with 46.64%wt. and O toms with 31.41%wt. are present in the chemical composition of the sample due to its magnetite phase. Finally, these images and EDS data completely prove the composition of Mn doped Fe_3O_4 nanoparticles/3D-N doped graphene for the electro-synthesized powder.

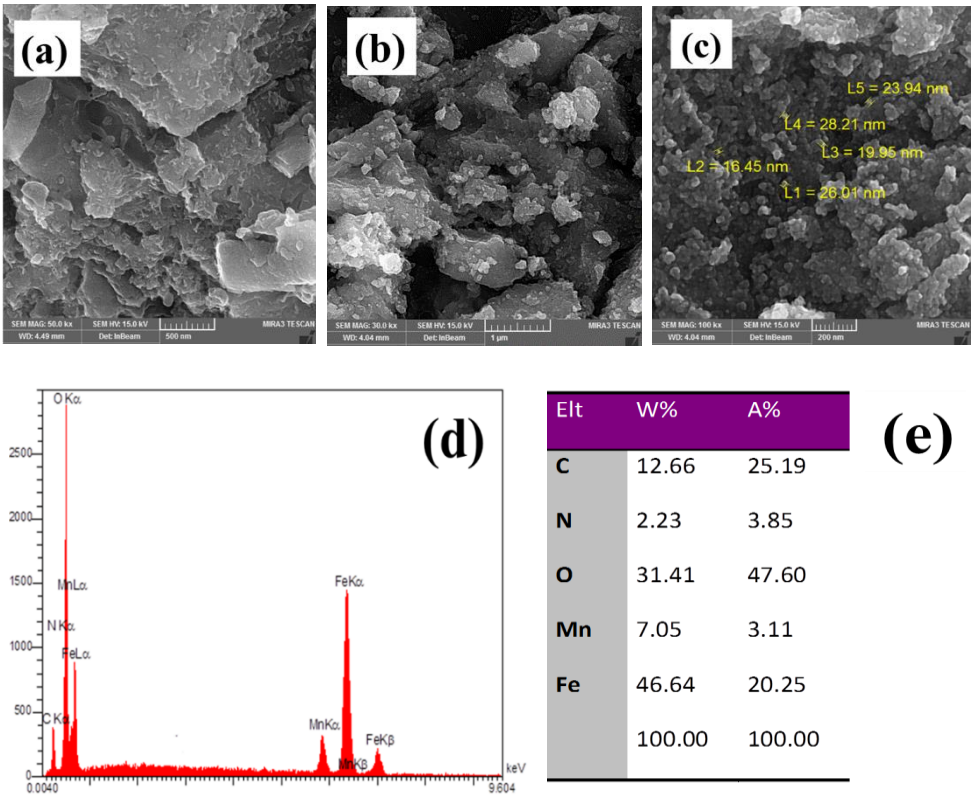

Elt	W%	A%
C	12.66	25.19
N	2.23	3.85
O	31.41	47.60
Mn	7.05	3.11
Fe	46.64	20.25
	100.00	100.00

Fig. FE-SEM images of (a) pure N-doped graphene and (b,c) its composite with iron oxide, and (d) elemental analysis profile and (e) the obtained EDS data

IR spectrum of the prepared composite is presented in Fig. 3. In the wavenumber range of 800-3500 cm^{-1}, there are several IR adsorption located at The spectrum exhibits six bands at 3447 cm^{-1}, 2922 cm^{-1}, 1624 cm^{-1}, 1465 cm^{-1}, 1382 cm^{-1}, 1338 cm^{-1}, 1272 cm^{-1}, 1176 cm^{-1}, 1027 cm^{-1} and 866 cm^{-1} (Fig. 3). The IR bands are due to the vibrations of following chemical bonds [63-67]; $\nu_{stretching}$ of N-H at 3447 cm^{-1}, $\nu_{asymmetric}$ stretching of -CH_2 at 2922 cm^{-1}, $\nu_{stretching}$ of O-H at 3500 cm^{-1}, $\nu_{stretching}$ of C=N at 1624 cm^{-1}, $\nu_{bending}$ of H_2O and 1624 cm^{-1}, $\nu_{scissoring}$ of CH_2 at 1462 cm^{-1}, $\nu_{stretching}$ of N-H at 1465 cm^{-1}, $\nu_{stretching}$ of C-N at 1382 cm^{-1}, $\nu_{wagging}$ of CH_2 at 1338 cm^{-1}, $\nu_{stretching}$ of carbon-oxygen at 1027 cm^{-1} and $\nu_{rocking}$ of CH_2 at 886 cm^{-1}. These IR adsorption bands indicate the presence of N-doped graphene in the prepared sample. On the other hand, there are four IR band at the wavenumbers below 700 cm^{-1} (inset in Fig. 3). The two adsorptions at 627 and 574 cm^{-1} are due to the Fe-O-Fe and/or Fe-O-Mn vibrations in tetrahedral sites [54]. And the next two bands at 462 and 429 cm^{-1} are related to the Fe-O-Fe vibration at octahedral sites in magnetite phase [68-70]. Hence, the magnetite presence in the prepared composite is also revealed form IR data.

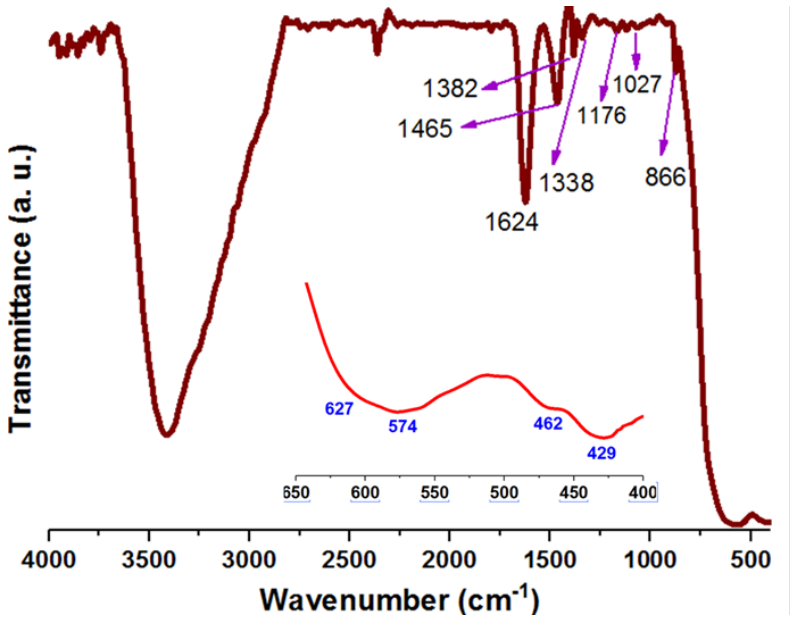

Fig. 3. IR spectrum of the prepared composite

The VSM curves of the synthesized nanocomposite at both conditions of high and low field zones are shown in Fig. 4. These curves have provided through recording magnetization values vs. applied field at the range between -20000Oe to +20000Oe. From Fig. 4a, it is observable that the composite exhibits superparamagnetic behavior at the applied fields, and has a relative high saturation magnetization *(Ms)* value. Furthermore, no hysteresis loop is seen in the VSM profile of the nanocomposite, confirming the suitable magnetic performance of Fe_3O_4 NPs grown 3D-N doped porous graphene. The magnetic behavior of the composite is also provided

at low fields, where the applied field near zero, as shown in Fig. 4b. The remanence values (both positive *Mr* and negative *Mr*) and the negative and positive coercivity (*Hci*) are specified on the VSM curve in Fig. 4b. It is found that the nanocomposite exhibits very low *Mr* and *Hci* values, proving the superparamagnetic behavior and its suitability for the potential applications. In Table 1, the observed magnetic data for the prepared nanocomposite are listed and compared with those reported for iron oxide nanoparticles.

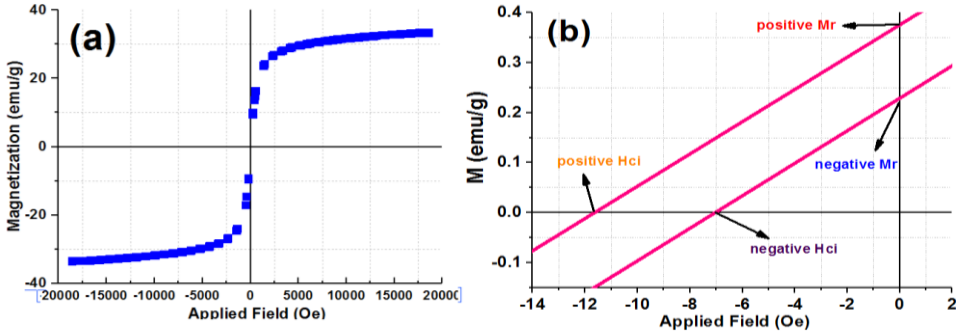

Fig. 4. Magnetization curve recorded through VSM analysis at (a) high applied field and (b) at field →0

Table 1. Comparison between the reported magnetic data of undoped magnetite NPs, Ni^{2+} doped MNPs and its GO composite.

Sample name [a]	Ms (emu/g)	Coercivity (Hci) G	Positive Hci (G)	Negative Hci (G)	Negative Mr (emu/g)	Positive Mr (emu/g)	Retentivity Mr (emu/g)	Ref.
Mn-IO/3D-N dope graphene	33.45	2.41	-11.65	-7.1	0.36	0.21	0.26	This work
Mn-doped iron oxide NPs	47.25	4.48	25.55	15.85	-1.15	-0.71	0.22	[61]
Un-doped iron oxide NPs	72.96	14.6	-41.87	-12.66	0.83	2.73	0.95	[71]
Ni-doped iron oide/ rGO	47.03	3.76	-9.15	-1.62	0.35	0.06	0.14	[72]

[a] Mn-IO indicates the Mn doped iron oxide NPs

Form the magnetic data listed for naked-IO, metal-ion doped IO and IO/3D-N doped graphene nanocomposite, the following facts are founded:

(i) The nanocomposite sample shows the relative small *Ms* value as compared with naked and Mn doped iron oxide NPs, which is related to non-magnetic part of the composite i.e. 3D-Ndoped graphene

(ii) The nanocomposite exhibits the lower coercivity value as compared with those of naked and Mn-doped IO NPs, revealing the improvement of superparamagnetic behavior of magnetite nanoparticles as a result of their composting with three dimensional N-doped porous graphene.

(iii) The nanocomposite has also lower *Mr* value (i.e. 0.26 emu/g) as compared with those of naked iron oxide NPs (i.e. Mr=0.95emu/g). This data proves an enhancement in the magnetic performance of iron oxide at low applied fields (field→0), which originate from the presence of 3D-N doped graphene, and single-domain behavior of the iron oxide nanoparticles.

4. CONCLUSION

In summary, a simple on-step electrochemical strategy was developed for the synthesis of superparamagnetic Mn^{2+}-doped iron oxide/ 3D nitrogen doped porous graphene. The magnetite crystal phase and particle morphology of the prepared composite was evidenced by XRD and FE-SEM analyses. The porous three-dimensional morphology and nitrogen content of the prepared graphene powder were also specified through FT-IR and EDS analyses, and microscopic observations. The fabricated powder showed superparamagnetic nature and an enhancement in its behaviour was observed due to Mn2+ doping and composition with porous N-doped graphene.

REFERENCES

[1] G. Reina, J.M. Gonzalez-Domınguez, A. Criado, E. Vazquez, A. Bianco, and M. Prato, Chem. Soc. Rev. 46 (2017) 4400.

[2] T.P. Dasari Shareena, D. McShan, A.K. Dasmahapatra, and P.B. Tchounwou, Nano-Micro Lett. 10 (2018) 53.

[3] J.S. Shayeh, A. Ehsani, M.R. Ganjali, P. Norouzi, and B. Jaleh, Appl. Surf. Sci. 353 (2015) 594.

[4] S. Priyadarsini, S. Mohanty, S. Mukherjee, S. Basu, and M. Mishra, J. Nanostruct. Chem. 8 (2018) 123.

[5] A. Ehsani, H.M. Shiri, E. Kowsari, R. Safari, J.S. Shayeh, and M. Barbary, J. Colloid Interface Sci. 490 (2017) 695.

[6] S.C. Jang, S.M. Kang, J.Y. Lee, S.Y. Oh, A.E. Vilian, and I. Lee, Int. J. Nanomed. 13 (2018) 221.

[7] E. Kowsari, A. Ehsani, M.D. Najafi, and M. Bigdeloo, J. Colloid Interface Sci. 512 (2018) 346.

[8] C. Chung, Y.K. Kim, D. Shin, S.R. Ryoo, B.H. Hong, and D.H. Min, Acc. Chem. Res. 46 (2013) 2211.

[9] A.N. Banerjee, Interface Focus 8 (2018) 20170056.

[10] S.S. Nanda, G.C. Papaefthymiou, and D.K. Yi, Critical Rev. Solid State Mater. Sci. 0 (2015)1.
[11] K. Yang, J. Wan, S. Zhang, B. Tian, Y. Zhang, and Z. Liu, Biomater. 33 (2012) 2206.
[12] D.P. Singh, C.E. Herrera, B. Singh, S. Singh, R.K. Singh, and R. Kumar, Mater. Sci. Eng. C 86 (2018) 173.
[13] H.M. Shiri, and M. Aghazadeh, J. Electrochem. Soc. 159 (2012) E132.
[14] M. Aghazadeh, M. Ghannadi Maragheh, and P. Norouzi, Int. J. Electrochem. Sci. 13 (2018) 1355.
[15] M. Rahimi-Nasrabadi, S.M. Pourmortazavi, M. Aghazadeh, M. R. Ganjali, M. Karimi, and P. Novrouzi. J. Mater. Sci.: Mater. Electron. 28 (2017) 3780.
[16] M. Aghazadeh, M. Ghaemi, A.N. Golikand, and A. Ahmadi, Mater. Lett. 65 (2011) 2545.
[17] M. Aghazadeh, and M.R. Ganjali, J. Mater. Sci. 53 (2018) 295.
[18] M. Rahimi-Nasrabadi, S.M. Pourmortazavi, M. Aghazadeh, M.R. Ganjali, M. Sadeghpour Karimi, and P. Novrouzi, J. Mater. Sci.: Mater. Electron. 28 (2017) 5574.
[19] M. Aghazadeh, and M.R. Ganjali, Ceram. Int. 44 (2018) 520.
[20] M. Aghazadeh, A.A.M. Barmi, and M. Hosseinifard, Mater. Lett. 73 (2012) 28.
[21] M. Rahimi-Nasrabadi, S. M. Pourmortazavi, M. Sadeghpour Karimi, M. Aghazadeh, M. R. Ganjali, and P. Norouzi, J. Mater. Sci.: Mater. Electron. 28 (2017) 13267.
[22] M. Aghazadeh, A.A.M. Barmi, H.M. Shiri, and S. Sedaghat, Ceram. Int. 39 (2013) 1045.
[23] M. Rahimi-Nasrabadi, S.M. Pourmortazavi, M. Aghazadeh, M. R. Ganjali, M. Sadeghpour Karimi, and P. Norouzi, J. Mater. Sci.: Mater. Electron. 28 (2017) 9478.
[24] M. Aghazadeh, J. Mater. Sci.: Mater. Electron. 28 (2016) 3108.
[25] M. Rahimi-Nasrabadi, S. M. Pourmortazavi, M. Sadeghpour Karimi, M. Aghazadeh, M. R. Ganjali, and P. Norouzi, J. Mater. Sci. Mater. Electron. 28 (2017) 6399.
[26] W. Wu, Z. Wu, T. Yu, C. Jiang, and W.S. Kim, Sci. Technol. Adv. Mater. 16 (2015) 023501.
[27] M. Hemmati, M. Rajabi, and A. Asghari, Mikrochim. Acta 185 (2018) 160.
[28] M.A. Gabal, K.M. Abou Zeid, A.A. El-Gendy, and M.S. El-Shall, J. Sol-Gel Sci. Technol. (2019) doi.org/10.1007/s10971-019-04917-4.
[29] D. Lisjak, and A. Mertelj, Prog. Mater. Sci. 95 (2018) 286.
[30] L. Mohammed, H.G. Gomaa, D. Ragab, and J. Zhu, Particuology 30 (2017) 1.
[31] M. Bilal, Y. Zhao, Tahir Rasheed, and Hafiz M.N. Iqbal, Int. J. Biol. Macromol. 120 (2018) 2530.
[32] S.M. Dadfara, K. Roemhild, N.I. Drude, S. Stillfried, R. Knüchel, F. Kiessling, and T. Lammers, Adv. Drug Delivery Rev. (2019) doi.org/10.1016/j.addr.2019.01.005.
[33] P.T. Yin, S. Shah, M. Chhowalla, and L.K.B. Design, Chem. Rev. 115 (2015) 2483.
[34] Y. Luo, Y. Tang, T. Liu, Q. Chen, X. Zhou, N. Wang, M. Ma, Y. Cheng, and H. Chen, Chem. Commun. 55 (2019) 1963.
[35] K. Movlaee, M.R. Ganjali, P. Norouzi, and G. Neri, Nanomater. 7 (2017) 406.

[36] K. Tadyszak, J.K. Wychowaniec, and J. Litowczenko, Nanomater. 8 (2018) 944.
[37] R. Justin, K. Tao, S. Román, D. Chen, Y. Xu, X. Geng, I.M. Ross, R.T. Grant, A. Pearson, G. Zhou, S.M. Neil, K. Sun, and B. Chen, Carbon 97 (2016) 54.
[38] N. Alegret, A. Criadoa, and M. Prato, Curr. Med. Chem. 24 (2017) 529.
[39] W.Y. Pan, C.Ch. Huang, T.T. Lin, H.Y. Hu, Nanomed. 12 (2016) 43.
[40] M.O. Aydogdu, N. Ekren, M. Suleymanoglu, and S. Erdem-Kuruca, Colloids Surf. B 172 (2018) 718.
[41] X. Fan, G. Jiao, W. Zhao, P. Jin, and X. Li, Nanoscale 5 (2013) 1143.
[42] W. Chen, Y. Peiwei, Y. Zhang, L. Zhang, Z. Deng, and Z. Zhang, ACS Appl. Mater. Interfaces 3 (2011) 4085.
[43] N. Chau, C. Mard-Moyon, K. Kostarelos, and A. Bianco, Biochem. Biophys. Res. Commun. 468 (2015) 454.
[44] X. Ma, H. Tao, K. Yang, L. Feng, L. Cheng, X. Shi, and Y. Li, Nano Res. 5 (2012) 199.
[45] M. Aghazadeh, Mater. Lett. 211 (2018) 225.
[46] M. Aghazadeh, I. Karimzadeh, and M.R. Ganjali, J. Electronic Mater. 47 (2018) 3026.
[47] M. Aghazadeh, and M.R. Ganjali, J. Mater. Sci.: Mater. Electron. 29 (2018) 4981.
[48] M. Aghazadeh, I. Karimzadeh, and M.R. Ganjali, Mater. Lett. 228 (2018) 137.
[49] M. Aghazadeh, I. Karimzadeh, and M.R. Ganjali, J. Mater. Sci.: Mater. Electron. 28 (2017) 19061.
[50] M. Aghazadeh, I. Karimzadeh, M.R. Ganjali, and M. Ghannadi Maragheh, J. Mater. Sci.: Mater. Electron. 29 (2018) 5163.
[51] M. Aghazadeh, and I. Karimzadeh, Curr. Nanosci. 14 (2018) 42.
[52] I. Karimzadeh, M. Aghazadeh, M.R. Ganjali, P. Norouzi, T. Doroudi, and P.H. Kolivand, Mater. Lett. 189 (2017) 290.
[53] M. Aghazadeh, and I. Karimzadeh, Mater. Res. Express 4 (2017) 105505.
[54] M. Aghazadeh, I. Karimzadeh, and M.R. Ganjali, Mater. Lett. 209 (2017) 450.
[55] M. Aghazadeh, I. Karimzadeh, and M.R. Ganjali, J. Mater. Sci.: Mater. Electron. 28 (2017) 13532.
[56] J. Tizfahm, M. Aghazadeh, M.G. Maragheh, M.R. Ganjali, P. Norouzi, and F. Faridbod, Mater. Lett. 167 (2016) 153.
[57] J. Talat Mehrabad, M. Aghazadeh, M. Ghannadi Maragheh, M.R. Ganjali, and P. Norouzi, Mater. Lett. 184 (2016) 223.
[58] I. Karimzadeh, H. Rezagholipour Dizaji, and M. Aghazadeh, Mater. Res. Express 3 (2016) 095022.
[59] D.C. Marcano, D.V. Kosynkin, J.M. Berlin, A. Sinitskii, Z. Sun, A. Slesarev, L.B. Alemany, W. Lu and J.M. Tour, ACS Nano 4 (2010) 4806.
[60] J. Li, J. Jiang, H. Feng, Z. Xu, S. Tang, P. Deng, and D. Qian, RSC Adv. 6 (2016) 31565.

[61] M. Aghazadeh, I. Karimzadeh, M.R. Ganjali, and A. Behzad, J. Mater. Sci.: Mater. Electron. 28 (2017) 18121.
[62] M. Aghazadeh, and M.R. Ganjali, J. Mater. Sci.: Mater. Electron. 29 (2018) 2291.
[63] F. Zheng, Y. Yang, and Q. Chen, Nature Commun. 5 (2014) Article No. 5261.
[64] M.P. Kumar, M.M. Raju, A. Arunchander, S. Selvaraj, G. Kalita, T.N. Narayanan, A.K. Sahu, and D.K. Pattanayak, J. Electrochem. Soc. 163 (2016) F848.
[65] Y. Gong, D. Li, Q. Fu, and C. Pan, Prog. Natural Sci. 25 (2015) 379.
[66] A. Ariharan, B. Viswanathan, V. Nandhakumar, Graphene 6 (2017) 41.
[67] Y. Li, D. Pan, M. Zhang, J. Xie, and Z. Yan, RSC Adv. 6 (2016) 48357.
[68] I. Karimzadeh, M. Aghazadeh, M.R. Ganjali, and T. Dourudi, Curr. Nanosci. 13 (2017) 167.
[69] M. Aghazadeh, J. Mater. Sci.: Mater. Electron. 28 (2017) 18755.
[70] I. Karimzadeh, M. Aghazadeh, T. Doroudi, M.R. Ganjali, P.H. Kolivand, and D. Gharailou, Curr. Nanosci. 13 (2017) 274.
[71] M. Aghazadeh, I. Karimzadeh, M. Ghannadi Maragheh, and M.R. Ganjali, Mater. Res. 21 (2018) e20180094.
[72] I. Karimzadeh, Anal. Bioanal. Electrochem. 10 (2018) 631.